On Passivity Characterization of Symmetric Rational Macromodels

(Article begins on next page)

On Passivity Characterization of Symmetric Rational Macromodels

Stefano Grivet-Talocia, *Senior Member, IEEE*

Abstract—This paper provides a theoretical framework for passivity characterization of symmetric rational macromodels. These may be obtained for linear and time-invariant reciprocal structures if structural symmetry is preserved during the rational fitting stage of the macromodel generation. Standard Hamiltonian-based methods can be used to characterize any passivity violation of such macromodels. Recent developments have suggested, however, that the same results may be obtained at a reduced computational cost, using so-called "half-size" passivity test matrices. In this paper, we generalize such results by providing a complete theoretical framework. In addition to imaginary Hamiltonian eigenvalues, we present a complete characterization of associated eigenvectors, allowing for precise localization of passivity violations. Since half-size matrices are also used for computing the eigenvectors, the overall computational cost is reduced up to a factor of eight. Several numerical examples validate and confirm the theoretical developments.

Index Terms—Admittance, Hamiltonian matrices, impedance, linear macromodeling, passivity, reciprocity, scattering, skew-Hamiltonian matrices, symmetry.

I. INTRODUCTION

RATIONAL macromodeling has become a standard approach for time-domain simulation of high-speed electronic circuits. Native characterization of electrical interconnects at chip, package, or board level, including both signal and power delivery networks, is typically available in the frequency domain in form of tabulated scattering, admittance, or impedance matrices, as a result of full-wave simulation or measurement. It is well known that the direct inclusion of such data into circuit-based system-level analysis flows poses serious numerical challenges [2]. Rational macromodeling provides a good solution to these problems. The frequency-domain samples are first processed by a rational fitting engine [3]–[9], leading to a closed-form representation of the transfer matrix in terms of poles and residues. This form is readily synthesized into an equivalent circuit, compatible with any SPICE-compatible circuit solver and ready for system-level analysis.

Passivity characterization and enforcement plays a crucial role in this process. If the macromodel is not passive, the transient simulation may become unstable and fail even if the model is terminated into passive networks [1], [2], [10], [15]. Therefore, significant efforts have been devoted in recent years for the development of robust and efficient passivity check and enforcement methods [15]–[27]. It is now widely recognized that one of the most reliable techniques is based on the spectral characterization of suitable Hamiltonian matrices [16], [23], [24], [28], [32], [33].

One of the main drawbacks of Hamiltonian-based techniques is the computational cost required for the extraction of the Hamiltonian eigenvalues/eigenvectors. This cost scales as the third power of the Hamiltonian matrix size, which, in turn, is twice the total number of poles of the macromodel. Thus, processing of large-scale macromodels may become quite demanding. Solutions for reducing this computational cost have been proposed in [15] and [25] by exploiting sparse structured state–space realizations within dedicated sparse eigensolvers.

The computational cost for Hamiltonian eigenvalue extraction may be reduced if the macromodel response is structurally symmetric. This is the case when the physical structure is reciprocal, and when symmetry is preserved during the rational fitting stage of the macromodel generation. For instance, one can fit with rational functions only the upper triangular part of the transfer matrix and copy the results into the lower triangular part. This process has both the advantages of preserving in the macromodel structure the constraints imposed by reciprocity, and of reducing the computational cost of macromodel derivation.

Recent developments [32], [33] have shown that the Hamiltonian eigenvalues required for passivity characterization of symmetric macromodels may be obtained by processing "half-size" passivity test matrices, leading to a reduction in the computational cost by a factor of eight. However, the main results in [32] and [33] are derived only for particular cases that are not clearly identified. One of the main objectives of this paper is indeed to provide a complete and self-consistent theoretical framework for the Hamiltonian-based passivity characterization of symmetric rational macromodels. It will be shown that four different passivity test matrices may be used, only one being Hamiltonian. All relations between these test matrices are fully developed here, including the general derivation of the "half-size" passivity test matrices of [32] and [33]. The latter are shown to provide a spectral factorization of the square of a full-size non-Hamiltonian passivity test matrix. In addition, this paper extends previous results by providing a complete characterization of Hamiltonian eigenvectors based on reduced-complexity eigendecompositions. These techniques may be used for the precise identification of passivity violation subbands at a reduced computational cost with respect to state-of-the-art methods.

II. PRELIMINARIES AND NOTATION

A. Basic Notation

We consider a general p-port linear and time-invariant structure. The input–output behavior of the structure is described via a Laplace-domain rational macromodel $\mathbf{H}(s)$ obtained via some fitting, approximation, or identification process.[1] Several algorithms are available for this task, including the well-known *vector fitting* scheme in its various implementations [3]–[9]. For the sake of generality, $\mathbf{H}(s)$ will denote either a scattering or a hybrid matrix, the latter including as particular cases both impedance and admittance representations.

It is well known [11] that any matrix of (proper) rational functions can be represented as

$$\mathbf{H}(s) = \mathbf{D} + \mathbf{C}(s\mathbf{I} - \mathbf{A})^{-1}\mathbf{B} \qquad (1)$$

where $\{\mathbf{A}, \mathbf{B}, \mathbf{C}, \mathbf{D}\}$ are the state–space matrices of some realization of $\mathbf{H}(s)$, and $\mathbf{I}$ is the identity matrix. Throughout this paper, no explicit structure will be considered for the state–space realization, and we will assume general complex-valued state–space matrices. We will, however, constrain the macromodel poles (eigenvalues of $\mathbf{A}$) to be stable with a strictly negative real part. Since $\mathbf{H}(s)$ represents a physical system, we also assume a real impulse response, which requires that

$$\mathbf{H}(s^*) = \mathbf{H}^*(s). \qquad (2)$$

B. Block-Structured Matrices

We are here interested in matrices with a particular block structure. Defining

$$\mathbf{J} = \begin{bmatrix} \mathbf{0} & \mathbf{I} \\ -\mathbf{I} & \mathbf{0} \end{bmatrix} \qquad (3)$$

we have the following classification [31] for $\mathcal{M} \in \mathbb{C}^{2n \times 2n}$:

$$\begin{aligned} \text{Hamiltonian}: & \quad (\mathcal{M}\mathbf{J})^H = +(\mathcal{M}\mathbf{J}) & (4) \\ \text{skew-Hamiltonian}: & \quad (\mathcal{M}\mathbf{J})^H = -(\mathcal{M}\mathbf{J}) & (5) \\ \text{J-symmetric}: & \quad (\mathcal{M}\mathbf{J})^T = +(\mathcal{M}\mathbf{J}) & (6) \\ \text{J-skew symmetric}: & \quad (\mathcal{M}\mathbf{J})^T = -(\mathcal{M}\mathbf{J}). & (7) \end{aligned}$$

For matrices with the above structure, the eigenvalues always come in pairs with specific symmetry constraints. In particular, if μ is an eigenvalue, we have

$$\begin{aligned} \text{Hamiltonian}: & \quad \{\mu, -\mu^*\} \in \text{eig}\{\mathcal{M}\} \\ \text{skew-Hamiltonian}: & \quad \{\mu, \mu^*\} \in \text{eig}\{\mathcal{M}\} \\ \text{J-symmetric}: & \quad \{\mu, -\mu\} \in \text{eig}\{\mathcal{M}\} \\ \text{J-skew symmetric}: & \quad \{\mu, \mu\} \in \text{eig}\{\mathcal{M}\}. \end{aligned}$$

This implies that the eigenspectrum of real-valued Hamiltonian matrices is symmetric with respect of both real and imaginary axes (four-quadrant symmetry), whereas all eigenvalues of real

[1] Throughout this paper, x, $\boldsymbol{x}$, and $\mathbf{X}$ denote a generic scalar, vector (lower case and boldface), and matrix (upper case and boldface), respectively. Superscripts *, ^{T}, and ^{H} will stand for the complex conjugate, transpose, and conjugate (Hermitian) transpose, respectively.

skew-Hamiltonian matrices have at least double (in general, even) multiplicity. It is straightforward to prove that when $\mathcal{M}$ is Hamiltonian (J-symmetric), then $\mathcal{M}^2$ is skew-Hamiltonian (J-skew symmetric).

C. Passivity Characterization

A system in the form (1) is passive when the following conditions are fulfilled [12]–[14]:
1) $\mathbf{H}(s)$ defined and analytic in $\mathbb{Re}\{s\} > 0$;
2) $\mathbf{H}(s^*) = \mathbf{H}^*(s)$;
3a) $\boldsymbol{\Psi}(s) \geq 0$, $\mathbb{Re}\{s\} > 0$ (hybrid representations);
3b) $\boldsymbol{\Phi}(s) \geq 0$, $\mathbb{Re}\{s\} > 0$ (scattering representations);
where

$$\boldsymbol{\Psi}(s) = \frac{1}{2}\left(\mathbf{H}(s) + \mathbf{H}^H(s)\right) \qquad (8)$$

$$\boldsymbol{\Phi}(s) = \left(\mathbf{I} - \mathbf{H}^H(s)\mathbf{H}(s)\right). \qquad (9)$$

For hybrid (admittance, impedance) representations, the nonnegativity condition 3a) is equivalent to requiring that all eigenvalues of $\boldsymbol{\Psi}(s)$ must be nonnegative for $\mathbb{Re}\{s\} > 0$. In the scattering case, condition 3b) is equivalent to the nonexpansivity (unitary boundedness) requirement that all singular values of $\mathbf{H}(s)$ must not exceed 1 for $\mathbb{Re}\{s\} > 0$. Note that conditions 1) and 2) are guaranteed by the working assumptions of model stability and real impulse response (2), and that conditions 3a) and 3b) may be restricted to the imaginary axis $s = j\omega$, as discussed in [14].

Throughout the following, we will assume that the model is asymptotically strictly passive, i.e.:

$$\mathbf{D} + \mathbf{D}^H > 0 \qquad (10)$$

for hybrid, admittance, and impedance representations, and

$$\mathbf{I} - \mathbf{D}^H\mathbf{D} > 0 \qquad (11)$$

for scattering representations. If this is not the case, asymptotic (strict) passivity can be achieved via perturbation using the techniques reported in [15] and [20].

It is widely acknowledged that the most reliable test for the above passivity conditions is based on the spectral characterization of Hamiltonian matrices [24], [28]. This test avoids checking conditions 3a) and 3b) via a brute-force frequency sampling process, which might be computationally expensive and inaccurate. We recall the definition of the Hamiltonian matrix corresponding to (1) (see the Appendix, Section A and [24] and [28]). In the hybrid (impedance and admittance) case, we have

$$\mathcal{N}_\delta = \begin{bmatrix} \mathbf{A} + \mathbf{B}\mathbf{Q}_\delta^{-1}\mathbf{C} & \mathbf{B}\mathbf{Q}_\delta^{-1}\mathbf{B}^H \\ -\mathbf{C}^H\mathbf{Q}_\delta^{-1}\mathbf{C} & -\mathbf{A}^H - \mathbf{C}^H\mathbf{Q}_\delta^{-1}\mathbf{B}^H \end{bmatrix} \qquad (12)$$

with $\mathbf{Q}_\delta = (2\delta\mathbf{I} - \mathbf{D} - \mathbf{D}^H)$, whereas in the scattering case, we have

$$\mathcal{M}_\gamma = \begin{bmatrix} \mathbf{A} - \mathbf{B}\mathbf{R}_\gamma^{-1}\mathbf{D}^H\mathbf{C} & -\gamma\mathbf{B}\mathbf{R}_\gamma^{-1}\mathbf{B}^H \\ \gamma\mathbf{C}^H\mathbf{S}_\gamma^{-1}\mathbf{C} & -\mathbf{A}^H + \mathbf{C}^H\mathbf{D}\mathbf{R}_\gamma^{-1}\mathbf{B}^H \end{bmatrix} \qquad (13)$$

with $\mathbf{R}_\gamma = (\mathbf{D}^H\mathbf{D} - \gamma^2\mathbf{I})$ and $\mathbf{S}_\gamma = (\mathbf{D}\mathbf{D}^H - \gamma^2\mathbf{I})$. We remark that definitions (12) and (13) are consistent for a generic

complex state–space realization, and that *only* in case of real state–space matrices, the conjugate-transpose operator ^{H} may be replaced by the transpose operator ^{T}. This fact has been the source of some confusion in the existing literature [32], [33], as will be discussed below.

The Hamiltonian-based passivity characterization [24], [28] is based on the presence of purely imaginary eigenvalues of matrices $\mathcal{N}_0$ (hybrid) or $\mathcal{M}_1$ (scattering). We have the following two theorems.

Theorem 1: Let $\mathbf{H}(s)$ be a macromodel in hybrid (admittance or impedance) form, defined by a state–space realization $\{\mathbf{A}, \mathbf{B}, \mathbf{C}, \mathbf{D}\}$. $j\omega_0$ is then a purely imaginary eigenvalue of $\mathcal{N}_\delta$ if and only if (iff) δ is an eigenvalue of $\mathbf{\Psi}(j\omega_0)$.

Theorem 2: Let $\mathbf{H}(s)$ be a macromodel in scattering form, defined by a state–space realization $\{\mathbf{A}, \mathbf{B}, \mathbf{C}, \mathbf{D}\}$. $j\omega_0$ is then a purely imaginary eigenvalue of $\mathcal{M}_\gamma$ iff γ is a singular value of $\mathbf{H}(j\omega_0)$.

A sketch of the proof for the above theorems is available in the Appendix, Section A.

Setting, as a particular case, $\delta = 0$ and $\gamma = 1$, we conclude that the (simple) imaginary Hamiltonian eigenvalues $j\omega_i$ pinpoint the frequencies at which one of the eigenvalues $\lambda(j\omega)$ of $\mathbf{\Psi}(j\omega)$ (hybrid, admittance, and impedance) or $\mathbf{\Phi}(j\omega)$ (scattering) changes sign. Therefore, if there are no purely imaginary Hamiltonian eigenvalues, all eigenvalues of $\mathbf{\Psi}(j\omega)$ (respectively, $\mathbf{\Phi}(j\omega)$) remain positive (due to the asymptotic strict passivity assumption), and the model is guaranteed passive. This fact is summarized in the following corollaries.

Corollary 1: Let $\mathbf{H}(s)$ be a macromodel in hybrid (admittance or impedance) form, defined by a state–space realization $\{\mathbf{A}, \mathbf{B}, \mathbf{C}, \mathbf{D}\}$ with $\mathbf{D} + \mathbf{D}^H > 0$. The macromodel is passive iff $\mathcal{N}_0$ has no purely imaginary eigenvalues.

Corollary 2: Let $\mathbf{H}(s)$ be a macromodel in scattering form, defined by a state–space realization $\{\mathbf{A}, \mathbf{B}, \mathbf{C}, \mathbf{D}\}$ with $\mathbf{I} - \mathbf{D}^H \mathbf{D} > 0$. The macromodel is passive iff $\mathcal{M}_1$ has no purely imaginary eigenvalues.

Fig. 1(a) depicts the eigenvalues of $\mathbf{\Psi}(j\omega)$ as functions of frequency for a nonpassive admittance model, highlighting the frequency bands where passivity violations occur. The dots in the panel of Fig. 1(a) depict the imaginary eigenvalues of the associated Hamiltonian matrix, whereas Fig. 1(b) reports the full Hamiltonian eigenspectrum. Since in this case a real state–space realization was used, the full four-quadrant symmetry of the Hamiltonian eigenvalue set holds.

Fig. 1 highlights that knowledge of the imaginary Hamiltonian eigenvalues alone is not sufficient to determine whether the model is passive within any prescribed subband. One of the main results in [24] states that the passivity characterization of each subband may be obtained with no ambiguity if the first-order derivatives ξ_i of the eigenvalue trajectories (as functions of frequency) are also known at the frequencies ω_i corresponding to imaginary Hamiltonian eigenvalues. We report for completeness the following theorem (the proof can be found in [24]).

Theorem 3: Let $\mathcal{P}_\epsilon$ denote the Hamiltonian matrix $\mathcal{N}_\epsilon$ for hybrid, admittance, and impedance representations or $\mathcal{M}_{1+\epsilon}$ for scattering representations. Let $\Omega = \{j\omega_i : j\omega_i \in \mathrm{eig}\{\mathcal{P}_0\}, 0 < \omega_i < \omega_{i+1}\}$ collect the (sorted) imaginary Hamiltonian eigen-
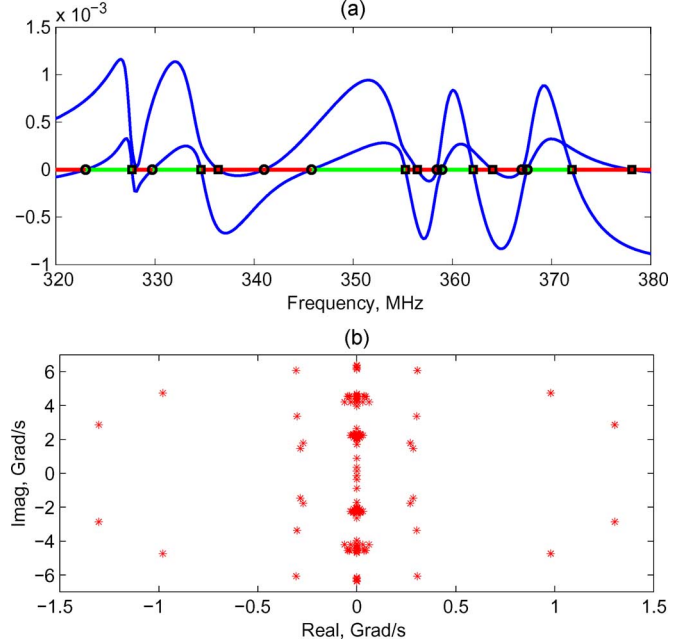

Fig. 1. (a) Eigenvalues (zoom) of $\mathbf{\Psi}(j\omega)$ for a nonpassive macromodel (solid lines) and frequencies corresponding to imaginary Hamiltonian eigenvalues (dots) (see also text). (b) Full Hamiltonian eigenspectrum.

values and let all these eigenvalues be simple. Finally, let ξ_i be defined as

$$\xi_i = \frac{j \boldsymbol{x}_i^H \boldsymbol{J} \boldsymbol{x}_i}{\boldsymbol{x}_i^H \boldsymbol{J} \mathcal{P}_0' \boldsymbol{x}_i} \tag{14}$$

where $\boldsymbol{x}_i$ is the right Hamiltonian eigenvector corresponding to $j\omega_i$, and $\mathcal{P}_0'$ is the first-order perturbation of the Hamiltonian matrix according to the expansion

$$\mathcal{P}_\epsilon = \mathcal{P}_0 + \epsilon \mathcal{P}_0' + \cdots. \tag{15}$$

$\boldsymbol{H}(j\omega)$ is then locally passive for $\omega \in (\omega_{i-1}, \omega_i)$ iff

$$\sum_{k \geq i} \mathrm{sgn}(\xi_k) = 0 \tag{16}$$

where $\mathrm{sgn}(\cdot)$ extracts the sign of its argument and $\omega_0 = 0$.

Remark 1: Theorem 3 shows that a precise passivity characterization also requires the eigenvectors $\boldsymbol{x}_i$ of the Hamiltonian matrix. Actually, most passivity enforcement schemes based on Hamiltonian eigenvalue perturbation make explicit use of these eigenvectors [15], [24]. One of the main objectives of this paper is to provide a complete characterization of both eigenvalues and eigenvectors for the specific case of symmetric macromodels.

III. PASSIVITY OF SYMMETRIC MACROMODELS

This work concentrates on passivity characterization of symmetric rational macromodels

$$\mathbf{H}^T(s) = \mathbf{H}(s). \tag{17}$$

Symmetric macromodels are obtained if: 1) the physical structure under investigation is reciprocal and 2) the adopted rational fitting scheme preserves structural symmetry in the macromodel. In addition to physical consistency, use of symmetric

macromodels is convenient since only the upper triangular portion of the transfer matrix needs to be processed by numerical fitting. Thus, a symmetric macromodel can be obtained at a reduced computational cost. We will only consider symmetric macromodels with real impulse response (2), denoted as *real symmetric* (even if corresponding to a complex state–space realization). For such models, the direct coupling matrix $\mathbf{D}$ must be such that

$$\mathbf{D} = \mathbf{D}^* = \mathbf{D}^T = \mathbf{D}^H. \tag{18}$$

The problem of passivity characterization of real-symmetric macromodels has been investigated by recent literature. The main results of [32] and [33] show that the set of imaginary eigenvalues Ω may be obtained by processing a so-called *half-size passivity matrix*, which is somewhat related to the classical Hamiltonian matrices. However, some of the derivations in [32] and [33] are flawed by minor inconsistenties and apply only in particular cases. In this work, we extend such results by providing a general derivation. In addition, we show all relevant connections with classical Hamiltonian methods. Finally, we provide a characterization of the Hamiltonian eigenvectors that is able to reduce by a factor of eight the computational cost with respect to the standard nonsymmetric case.

A. Passivity Matrices: Hamiltonian or Non-Hamiltonian?

The conjugate (Hermitian) transpose of a generic (unstructured) macromodel is expressed as

$$\mathbf{H}^H(s) = \mathbf{D}^H + \mathbf{B}^H(s^*\mathbf{I} - \mathbf{A}^H)^{-1}\mathbf{C}^H. \tag{19}$$

Using this representation in (8) and (9) leads to the standard Hamiltonian passivity characterization results of Section II-C. However, in case of a real-symmetric model, we have three additional representations

$$\mathbf{H}^H(s) = \mathbf{H}(s^*) = \mathbf{D} + \mathbf{C}(s^*\mathbf{I} - \mathbf{A})^{-1}\mathbf{B} \tag{20}$$
$$= \mathbf{H}^T(s^*) = \mathbf{D} + \mathbf{B}^T(s^*\mathbf{I} - \mathbf{A}^T)^{-1}\mathbf{C}^T \tag{21}$$
$$= \mathbf{H}^*(s) = \mathbf{D} + \mathbf{C}^*(s^*\mathbf{I} - \mathbf{A}^*)^{-1}\mathbf{B}^*. \tag{22}$$

which, in turn, lead to the alternative definitions

$$\mathbf{\Psi}(s) = \widehat{\mathbf{\Psi}}(s) = \frac{1}{2}\left(\mathbf{H}(s) + \mathbf{H}(s^*)\right) \tag{23}$$
$$= \overline{\mathbf{\Psi}}(s) = \frac{1}{2}\left(\mathbf{H}(s) + \mathbf{H}^T(s^*)\right) \tag{24}$$
$$= \widetilde{\mathbf{\Psi}}(s) = \frac{1}{2}\left(\mathbf{H}(s) + \mathbf{H}^*(s)\right) \tag{25}$$

and

$$\mathbf{\Phi}(s) = \widehat{\mathbf{\Phi}}(s) = (\mathbf{I} - \mathbf{H}(s^*)\mathbf{H}(s)) \tag{26}$$
$$= \overline{\mathbf{\Phi}}(s) = (\mathbf{I} - \mathbf{H}^T(s^*)\mathbf{H}(s)) \tag{27}$$
$$= \widetilde{\mathbf{\Phi}}(s) = (\mathbf{I} - \mathbf{H}^*(s)\mathbf{H}(s)). \tag{28}$$

These may be used instead of (8) and (9) to characterize the macromodel passivity as in Section II-C. Indeed, following the

same steps of Appendix A, definitions (23)–(25) lead, respectively, to the three new passivity characterization matrices

$$\widehat{\mathcal{N}}_\delta = \begin{bmatrix} \mathbf{A} + \mathbf{B}\widehat{\mathbf{Q}}_\delta^{-1}\mathbf{C} & \mathbf{B}\widehat{\mathbf{Q}}_\delta^{-1}\mathbf{C} \\ -\mathbf{B}\widehat{\mathbf{Q}}_\delta^{-1}\mathbf{C} & -\mathbf{A} - \mathbf{B}\widehat{\mathbf{Q}}_\delta^{-1}\mathbf{C} \end{bmatrix} \tag{29}$$

$$\overline{\mathcal{N}}_\delta = \begin{bmatrix} \mathbf{A} + \mathbf{B}\widehat{\mathbf{Q}}_\delta^{-1}\mathbf{C} & \mathbf{B}\widehat{\mathbf{Q}}_\delta^{-1}\mathbf{B}^T \\ -\mathbf{C}^T\widehat{\mathbf{Q}}_\delta^{-1}\mathbf{C} & -\mathbf{A}^T - \mathbf{C}^T\widehat{\mathbf{Q}}_\delta^{-1}\mathbf{B}^T \end{bmatrix} \tag{30}$$

$$\widetilde{\mathcal{N}}_\delta = \begin{bmatrix} \mathbf{A} + \mathbf{B}\widehat{\mathbf{Q}}_\delta^{-1}\mathbf{C} & \mathbf{B}\widehat{\mathbf{Q}}_\delta^{-1}\mathbf{C}^* \\ -\mathbf{B}^*\widehat{\mathbf{Q}}_\delta^{-1}\mathbf{C} & -\mathbf{A}^* - \mathbf{B}^*\widehat{\mathbf{Q}}_\delta^{-1}\mathbf{C}^* \end{bmatrix} \tag{31}$$

where $\widehat{\mathbf{Q}}_\delta = 2(\delta\mathbf{I} - \mathbf{D})$, for admittance or impedance representations, while definitions (26)–(28) lead to

$$\widehat{\mathcal{M}}_\gamma = \begin{bmatrix} \mathbf{A} - \mathbf{B}\mathbf{D}\widehat{\mathbf{R}}_\gamma^{-1}\mathbf{C} & -\gamma\mathbf{B}\widehat{\mathbf{R}}_\gamma^{-1}\mathbf{C} \\ \gamma\mathbf{B}\widehat{\mathbf{R}}_\gamma^{-1}\mathbf{C} & -\mathbf{A} + \mathbf{B}\mathbf{D}\widehat{\mathbf{R}}_\gamma^{-1}\mathbf{C} \end{bmatrix} \tag{32}$$

$$\overline{\mathcal{M}}_\gamma = \begin{bmatrix} \mathbf{A} - \mathbf{B}\mathbf{D}\widehat{\mathbf{R}}_\gamma^{-1}\mathbf{C} & -\gamma\mathbf{B}\widehat{\mathbf{R}}_\gamma^{-1}\mathbf{B}^T \\ \gamma\mathbf{C}^T\widehat{\mathbf{R}}_\gamma^{-1}\mathbf{C} & -\mathbf{A}^T + \mathbf{C}^T\mathbf{D}\widehat{\mathbf{R}}_\gamma^{-1}\mathbf{B}^T \end{bmatrix} \tag{33}$$

$$\widetilde{\mathcal{M}}_\gamma = \begin{bmatrix} \mathbf{A} - \mathbf{B}\mathbf{D}\widehat{\mathbf{R}}_\gamma^{-1}\mathbf{C} & -\gamma\mathbf{B}\widehat{\mathbf{R}}_\gamma^{-1}\mathbf{C}^* \\ \gamma\mathbf{B}^*\widehat{\mathbf{R}}_\gamma^{-1}\mathbf{C} & -\mathbf{A}^* + \mathbf{B}^*\mathbf{D}\widehat{\mathbf{R}}_\gamma^{-1}\mathbf{C}^* \end{bmatrix} \tag{34}$$

with $\widehat{\mathbf{R}}_\gamma = (\mathbf{D}^2 - \gamma^2\mathbf{I})$ for scattering representations. Any of the above matrices, together with (12) and (13), will be denoted as a "passivity" matrix. It is straightforward to prove the following Lemmas.

Lemma 1: Let $\mathbf{H}(s)$ be a real-symmetric macromodel in admittance or impedance form, defined by a state–space realization $\{\mathbf{A}, \mathbf{B}, \mathbf{C}, \mathbf{D}\}$. The matrices $\mathcal{N}_\delta, \widehat{\mathcal{N}}_\delta, \overline{\mathcal{N}}_\delta$, and $\widetilde{\mathcal{N}}_\delta$ are then similar and share the same set of eigenvalues.

Lemma 2: Let $\mathbf{H}(s)$ be a real-symmetric macromodel in scattering form, defined by a state–space realization $\{\mathbf{A}, \mathbf{B}, \mathbf{C}, \mathbf{D}\}$. The matrices $\mathcal{M}_\gamma, \widehat{\mathcal{M}}_\gamma, \overline{\mathcal{M}}_\gamma$, and $\widetilde{\mathcal{M}}_\gamma$ are then similar and share the same set of eigenvalues.

The proof is omitted since it follows the same steps reported in the Appendix, Section A after replacing the purely imaginary eigenvalue $j\omega_0$ with a generic $\mu \in \mathbb{C}$.

Remark 2: Matrices $\mathcal{N}_\delta$ and $\mathcal{M}_\gamma$ are Hamiltonian according to the classification of Section II-B for any complex-valued state–space realization.

Remark 3: Matrices $\overline{\mathcal{N}}_\delta$ and $\overline{\mathcal{M}}_\gamma$ are J-symmetric according to the classification of Section II-B for any complex-valued state–space realization. In general, $\overline{\mathcal{N}}_\delta$ and $\overline{\mathcal{M}}_\gamma$ are *not* Hamiltonian. This is somewhat misinterpreted in [33], where the distinction between real or complex-valued realizations and the Hamiltonian or J-symmetric structure is not well developed.

Remark 4: In case of a purely real state–space realization, the ^{H} and ^{T} operators coincide so that $\overline{\mathcal{N}}_\delta = \mathcal{N}_\delta$ and $\overline{\mathcal{M}}_\gamma = \mathcal{M}_\gamma$ are Hamiltonian and J-symmetric at the same time.

Remark 5: In case of (complex-valued) strictly symmetric state–space realizations (as defined in [33] with $\mathbf{A}$ diagonal and $\mathbf{B} = \mathbf{C}^T$), one can prove that $\widetilde{\mathcal{N}}_\delta$ and $\widetilde{\mathcal{M}}_\gamma$ are Hamiltonian, whereas $\widehat{\mathcal{N}}_\delta$ and $\widehat{\mathcal{M}}_\gamma$ are J-symmetric.

Combining the statements of Remarks 2 and 3 with the similarity considerations of Lemmas 1 and 2, we conclude that the full eigenvalue set Λ of all above-defined passivity matrices fulfills the symmetry constraints imposed by both the Hamiltonian

and J-symmetric structure. In particular, if μ is an eigenvalue, we have

$$\mu \in \mathbb{R} \quad \Rightarrow \quad \{\mu, -\mu\} \in \Lambda \tag{35}$$

$$\mu \in j\mathbb{R} \quad \Rightarrow \quad \{\mu, -\mu\} \in \Lambda \tag{36}$$

$$\mu \notin \mathbb{R} \cup j\mathbb{R} \quad \Rightarrow \quad \{\mu, -\mu, \mu^*, -\mu^*\} \in \Lambda. \tag{37}$$

This is true for any real-symmetric macromodel defined by a general complex-valued state–space realization. Thus, the constraints imposed by symmetry (17) add an additional structure to the classical eigenvalue symmetries listed in Section II-B.

B. Passivity Characterization of Real-Symmetric Macromodels

Any of the passivity matrices defined in Section III-A may be used to perform a purely algebraic passivity test of a real-symmetric macromodel. In particular, we can state the following theorems, which generalize Theorems 1 and 2 for the specific case of real-symmetric macromodels.

Theorem 4: Let $\mathbf{H}(s)$ be a real-symmetric macromodel in admittance or impedance form, defined by a state–space realization $\{\mathbf{A}, \mathbf{B}, \mathbf{C}, \mathbf{D}\}$. δ is then an eigenvalue of $\mathbf{\Psi}(j\omega_0)$ iff $j\omega_0$ is a purely imaginary eigenvalue of $\mathcal{N}_\delta, \widehat{\mathcal{N}}_\delta, \overline{\mathcal{N}}_\delta$, or $\widetilde{\mathcal{N}}_\delta$.

Theorem 5: Let $\mathbf{H}(s)$ be a real-symmetric macromodel in scattering form, defined by a state–space realization $\{\mathbf{A}, \mathbf{B}, \mathbf{C}, \mathbf{D}\}$. γ is then a singular value of $\mathbf{H}(j\omega_0)$ iff $j\omega_0$ is a purely imaginary eigenvalue of $\mathcal{M}_\gamma, \widehat{\mathcal{M}}_\gamma, \overline{\mathcal{M}}_\gamma$, or $\widetilde{\mathcal{M}}_\gamma$.

The Appendix, Section B reports a sketch of the proof for the cases $\widehat{\mathcal{N}}_\delta$ and $\widehat{\mathcal{M}}_\gamma$, which are of particular interest due to their structure, as discussed below. We conclude this section by noting that any of the passivity matrices above may be used to ascertain whether purely imaginary eigenvalues are present through Corollaries 1 and 2. If no such eigenvalues are found, the model is passive. Otherwise, a more precise characterization is needed.

C. Squared and Half-Size Passivity Matrices

Let $\mathcal{P}$ denote any of the above-defined passivity matrices, and let Λ be the set of its eigenvalues. We consider now the set of eigenvalues of $\mathcal{P}^2$, denoted as Λ_2. Obviously, we have

$$\mu \in \Lambda \quad \Rightarrow \quad \mu^2 \in \Lambda_2. \tag{38}$$

It can be shown that the set Λ_2 inherits both symmetry constraints imposed by the skew-Hamiltonian and J-skew symmetric structure. In particular, all eigenvalues of $\mathcal{P}^2$ have (at least) double multiplicity and are symmetric with respect to the real axis since for any $\lambda \in \Lambda_2$,

$$\lambda \in \mathbb{R} \quad \Rightarrow \quad \{\lambda, \lambda\} \in \Lambda_2 \tag{39}$$

$$\lambda \notin \mathbb{R} \quad \Rightarrow \quad \{\lambda, \lambda, \lambda^*, \lambda^*\} \in \Lambda_2. \tag{40}$$

Real negative eigenvalues $\lambda = -\omega_i^2$ are of particular interest for passivity characterization. In fact, these are obtained as the square of each pair of purely imaginary eigenvalues $\mu_i^\pm = \pm j\omega_i$ of $\mathcal{P}$. Obviously, due to the spectral symmetries imposed by

the realness condition (2), passivity characterization only requires detailed information on $\mu_i^+ = +j\omega_i$. Therefore, it is desirable to perform a spectral factorization of $\mathcal{P}^2$ in order to extract only those (simple) eigenvalues with associated eigenvectors that are of interest at a reduced computational cost. This is indeed one of the main achievements of [32] and [33], where a so-called "half-size" passivity test matrix was derived for admittance and scattering representations, respectively. We first recall these results, showing the particular connection with the above-defined passivity matrices $\mathcal{P}$. We then extend these results by also providing a reduced-complexity eigenvector characterization. Finally, we derive a complete passivity characterization of real-symmetric macromodels.

It was noted in [33] that the Hamiltonian matrix of a real-symmetric macromodel has a block structure

$$\begin{bmatrix} \mathbf{E} & \mathbf{F} \\ -\mathbf{F} & -\mathbf{E} \end{bmatrix}. \tag{41}$$

This is actually not true in general since the above structure only applies to matrices $\widehat{\mathcal{N}}_\delta$ and $\widehat{\mathcal{M}}_\gamma$ of (29) and (32), which are not Hamiltonian, as discussed in Section III-A. Restricting our analysis to these two passivity matrices, denoted collectively as $\widehat{\mathcal{P}}$, and defining

$$\mathbf{T} = \mathbf{T}^T = \mathbf{T}^{-1} = \frac{1}{\sqrt{2}} \begin{bmatrix} \mathbf{I} & \mathbf{I} \\ \mathbf{I} & -\mathbf{I} \end{bmatrix} \tag{42}$$

we see that

$$\widehat{\mathcal{P}}_T = \mathbf{T}\widehat{\mathcal{P}}\mathbf{T} = \begin{bmatrix} \mathbf{0} & \mathbf{\Theta}_+ \\ \mathbf{\Theta}_- & \mathbf{0} \end{bmatrix} \tag{43}$$

where

$$\mathbf{\Theta}_\pm = \mathbf{A} - \mathbf{B}(\mathbf{D} \pm \gamma\mathbf{I})^{-1}\mathbf{C} \tag{44}$$

in the scattering case, and

$$\mathbf{\Theta}_+ = \mathbf{A} \tag{45}$$

$$\mathbf{\Theta}_- = \mathbf{A} - \mathbf{B}(\mathbf{D} - \delta\mathbf{I})^{-1}\mathbf{C} \tag{46}$$

in the admittance and impedance cases. Taking the square of $\widehat{\mathcal{P}}_T$ leads to

$$\widehat{\mathcal{P}}_T^2 = \begin{bmatrix} \mathbf{P}_+ & \mathbf{0} \\ \mathbf{0} & \mathbf{P}_- \end{bmatrix} \tag{47}$$

where

$$\mathbf{P}_+ = \mathbf{\Theta}_+\mathbf{\Theta}_- \quad \text{and} \quad \mathbf{P}_- = \mathbf{\Theta}_-\mathbf{\Theta}_+. \tag{48}$$

It is straightforward to prove that

Lemma 3: Matrices $\mathbf{P}_+$ and $\mathbf{P}_-$ are similar.

Matrices $\mathbf{P}_+$ and $\mathbf{P}_-$ are denoted as *half-size passivity test matrices* in [32] and [33]. Due to its block-diagonal structure, the representation (47) provides a spectral factorization of $\widehat{\mathcal{P}}_T^2$. The full set of eigenvalues of any passivity matrix $\mathcal{P}$ is thus obtained by taking the two complex square roots of the eigenvalues of $\mathbf{P}_+$ (or $\mathbf{P}_-$). Furthermore, the critical frequencies ω_i required for passivity characterization, as discussed in Section II-B, are

simply determined from the restricted set of real negative eigenvalues $\lambda_i = -\omega_i^2$ of $\mathbf{P}_+$ or $\mathbf{P}_-$. This procedure allows a reduction of the computing time required by eigenvalue determination by a factor of eight [29].

D. Full-Size and Half-Size Eigenvectors

In this section, we also show that the eigenvectors of the full-size passivity matrices $\widehat{\mathcal{P}}$ can be obtained from the corresponding eigenvectors of the "half-size" matrices $\mathbf{P}_\pm$, leading to a reduction of computing time by a factor of eight. Section III-E will apply these results to the derivation of true Hamiltonian eigenvectors and passivity characterization. We have the following result (the proof is omitted).

Lemma 4: Let $\mathbf{w}_i^\pm$ be eigenvectors of $\mathbf{P}_\pm$ corresponding to a common eigenvalue λ_i. Then,

$$\mathbf{w}_i^- = \alpha \mathbf{\Theta}_- \mathbf{w}_i^+ \text{ and } \mathbf{w}_i^+ = \beta \mathbf{\Theta}_+ \mathbf{w}_i^- \tag{49}$$

where α and β are arbitrary nonvanishing complex constants. Considering a real negative eigenvalue $\lambda_i = -\omega_i^2$, we can apply this Lemma to extract the 2-D subspace of $\widehat{\mathcal{P}}_T$ corresponding to the eigenvalues $\pm j\omega_i$ via

$$\widehat{\mathcal{P}}_T \begin{bmatrix} \mathbf{w}_i^+ & \mathbf{0} \\ \mathbf{0} & \mathbf{w}_i^- \end{bmatrix} = \begin{bmatrix} \mathbf{0} & \mathbf{\Theta}_+ \mathbf{w}_i^- \\ \mathbf{\Theta}_- \mathbf{w}_i^+ & \mathbf{0} \end{bmatrix}$$
$$= \begin{bmatrix} \mathbf{0} & \mathbf{\Theta}_+ \mathbf{\Theta}_- \mathbf{w}_i^+ \\ \mathbf{w}_i^- & \mathbf{0} \end{bmatrix}$$
$$= \begin{bmatrix} \mathbf{w}_i^+ & \mathbf{0} \\ \mathbf{0} & \mathbf{w}_i^- \end{bmatrix} \begin{bmatrix} 0 & -\omega_i^2 \\ 1 & 0 \end{bmatrix} \tag{50}$$

where the first relation in (49) with $\alpha = 1$ has been used. The two eigenvectors corresponding to the individual eigenvalues $\pm j\omega_i$ are now readily obtained by diagonalizing the 2×2 matrix appearing last in (50). The result is

$$\widehat{\mathcal{P}}_T \begin{bmatrix} \pm j\omega_i \mathbf{w}_i^+ \\ \mathbf{\Theta}_- \mathbf{w}_i^+ \end{bmatrix} = \pm j\omega_i \begin{bmatrix} \pm j\omega_i \mathbf{w}_i^+ \\ \mathbf{\Theta}_- \mathbf{w}_i^+ \end{bmatrix}. \tag{51}$$

Finally, we can recover the eigenvectors $\widehat{\mathbf{w}}_i^\pm$ of the passivity matrix $\widehat{\mathcal{P}}$

$$\widehat{\mathcal{P}} \widehat{\mathbf{x}}_i^\pm = \pm j\omega_i \widehat{\mathbf{x}}_i^\pm \tag{52}$$

via similarity transformation (42) combined with (51), obtaining the two alternative representations

$$\widehat{\mathbf{x}}_i^\pm = \begin{bmatrix} (\pm j\omega_i \mathbf{I} + \mathbf{\Theta}_-) \mathbf{w}_i^+ \\ (\pm j\omega_i \mathbf{I} - \mathbf{\Theta}_-) \mathbf{w}_i^+ \end{bmatrix} \tag{53}$$

and

$$\widehat{\mathbf{x}}_i^\pm = \begin{bmatrix} (\pm j\omega_i \mathbf{I} + \mathbf{\Theta}_+) \mathbf{w}_i^- \\ (\mp j\omega_i \mathbf{I} + \mathbf{\Theta}_+) \mathbf{w}_i^- \end{bmatrix}. \tag{54}$$

E. Passivity Characterization via Half-Size Eigenvectors

Our aim here is to compute the (right) eigenvectors $\mathbf{x}_i$ of the Hamiltonian matrix $\mathcal{N}_0$ or $\mathcal{M}_1$ starting from the information available in the Half-size eigenvectors (53) or (54). Once $\mathbf{x}_i$ is available, straightforward application of Theorem 3 will lead

to global passivity characterization. We analyze separately the different macromodel representations.

1) Admittance and Impedance Representations: The full-size eigenvector of $\mathcal{N}_0$ corresponding to a purely imaginary eigenvalue $j\omega_i$ is provided by (67), where $\mathbf{r}$ and $\mathbf{q}$ are defined in (64) and (65) in terms of the relevant eigenvector $\mathbf{v}$ of $\mathbf{\Psi}(j\omega_i)$ (see the Appendix, Section A). However, $\mathbf{v}$ is also expressed via (77) in terms of the block components of $\widehat{\mathbf{w}}_i^+$, available in (53) or (54). A direct substitution leads to the two alternative expressions

$$\mathbf{x}_i^+ = \begin{bmatrix} \mathbf{K}_1^+ \\ \mathbf{K}_2^+ \end{bmatrix} \mathbf{w}_i^+ \text{ or } \mathbf{x}_i^+ = \begin{bmatrix} \mathbf{K}_1^- \\ \mathbf{K}_2^- \end{bmatrix} \mathbf{w}_i^-. \tag{55}$$

where the block matrices $\mathbf{K}_\nu^\pm$ depend only on the state–space matrices of the macromodel.

2) Scattering Representations: The same procedure used above for hybrid representations can be applied with minor modifications to the scattering case. In particular, the full-size eigenvector of $\mathcal{M}_1$ corresponding to a purely imaginary eigenvalue $j\omega_i$ is provided by (73), where $\mathbf{r}$ and $\mathbf{q}$ are defined in (70) and (71) in terms of the left and right singular vectors $\mathbf{u}$ and $\mathbf{v}$ of $\mathbf{H}(j\omega_i)$ (see the Appendix, Section A). Also in this case, $\mathbf{u}$ and $\mathbf{v}$ are expressed via (83) in terms of the block components of $\widehat{\mathbf{w}}_i^+$, available in (53) or (54). Therefore, the same Hamiltonian eigenvector representations (55) holds for the scattering case as well.

Let us now consider Theorem 3, and particularly the definition of the slopes ξ_i in (14). Using (55), we can easily derive the following compact characterization:

$$\xi_i = \frac{j\mathbf{w}_i^H \mathbf{\Gamma} \mathbf{w}_i}{\mathbf{w}_i^H \mathbf{\Delta} \mathbf{w}_i} \tag{56}$$

where the $\pm$ superscript has been omitted. Matrices $\mathbf{\Delta}$ and $\mathbf{\Gamma}$ can be shown to be Hermitian and skew-Hermitian, respectively. Therefore, ξ_i is real and still corresponds to the slope of the frequency-dependent eigenvalue/singular value that crosses the passivity threshold at $j\omega_i$. Expression (56), which is one of the main results in this paper, does not require the numeric computation of the invariant subspaces of the full-size Hamiltonian matrix, being defined by the half-size (right) eigenvector $\mathbf{w}_i$ of $\mathbf{P}_\pm$ of (48). As a consequence, the total computation time required for ξ_i is reduced by at most a factor of eight since the cost of a full eigendecomposition scales as the third power of the matrix size. The numerical results of Section IV will confirm this statement.

IV. EXAMPLES

A. Similarity of Passivity Test Matrices

The first example validates Lemma 2 on the following three test cases:

A) model of a 20-port via field under a land-grid array (LGA) connector (30-GHz bandwidth, 30 poles per response);

B) same as A, but with 50 poles per response;

C) six-port model of a coupled signal/power delivery structure (3-GHz bandwidth, 80 poles per response).

TABLE I
NUMERICAL VERIFICATION OF LEMMA 2 FOR THREE REAL-SYMMETRIC
RATIONAL MACROMODELS. SEE TEXT FOR A DETAILED DESCRIPTION

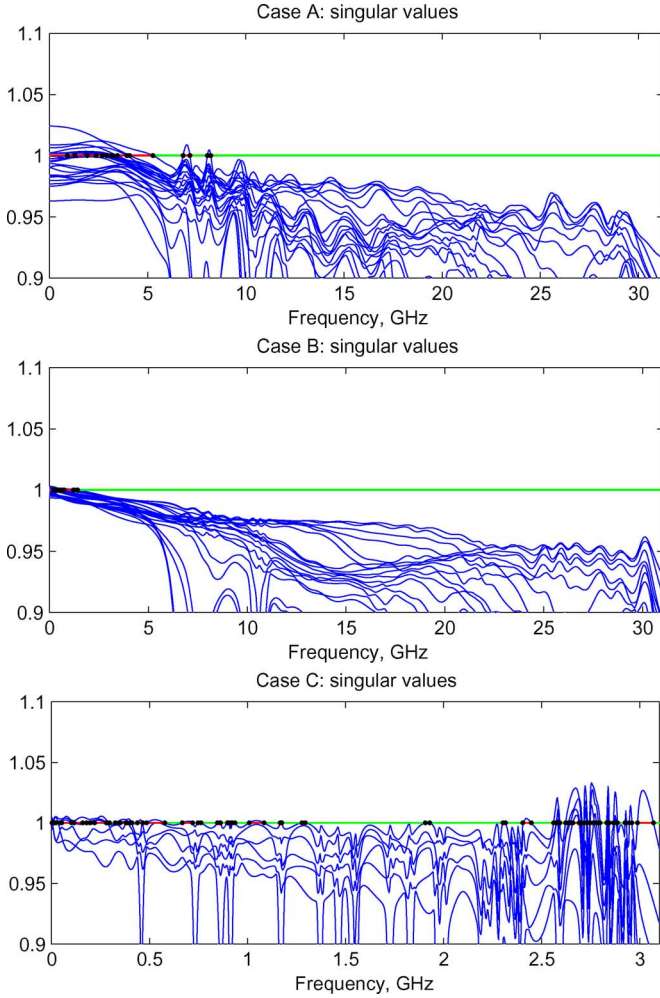| Case	n	p	n_i	$\varepsilon_{\widehat{\mathcal{P}}} = \varepsilon_{\widetilde{\mathcal{P}}}$	$\varepsilon_{\overline{\mathcal{P}}}$	$\varepsilon_{\text{half}}$
A	600	20	16	1.0×10^{-13}	0	2.5×10^{-12}
B	1000	20	8	1.1×10^{-12}	0	3.4×10^{-11}
C	450	6	93	1.3×10^{-12}	0	1.2×10^{-10}

Fig. 2. Singular values of $\mathbf{H}(j\omega)$ for three nonpassive macromodels (solid blue lines in online version) and frequencies corresponding to imaginary Hamiltonian eigenvalues (black dots).

A more detailed description of these structures is available in [15]. For each test case, a real-symmetric rational macromodel in scattering form has been obtained via vector fitting [3]. Table I summarizes the dynamic order n (size of state–space matrix $\mathbf{A}$), the number of ports p, and the number of imaginary Hamiltonian eigenvalues n_i. The three panels of Fig. 2 depict the singular values versus frequency, highlighting with black dots the frequencies of the purely imaginary Hamiltonian eigenvalues providing the crossing points of the unit threshold.

The four passivity matrices $\mathcal{M}_1$, $\widehat{\mathcal{M}}_1$, $\overline{\mathcal{M}}_1$, and $\widetilde{\mathcal{M}}_1$ have been constructed for all cases. We now compare the full set of eigenvalues of these matrices, which should coincide according to Lemma 2. The results are summarized in Table I. Denoting

with $\Lambda\{\mathcal{P}\}$ the full set of eigenvalues of matrix $\mathcal{P}$, we measure the deviation between two eigenvalue sets via the Hausdorff distance, defined as [34]

$$\mathcal{D}(\Lambda_1, \Lambda_2) = \max\left\{\text{dist}(\Lambda_1, \Lambda_2), \text{dist}(\Lambda_2, \Lambda_1)\right\} \quad (57)$$

where

$$\text{dist}(\Lambda_1, \Lambda_2) = \max\left\{\text{d}(\lambda, \Lambda_2), \lambda \in \Lambda_1\right\} \quad (58)$$

represents the one-sided distance between set Λ_1 and set Λ_2, and

$$\text{d}(\lambda, \Lambda) = \min\left\{|\lambda - \mu|, \mu \in \Lambda\right\} \quad (59)$$

represents the distance between complex point λ and the set Λ. The Hausdorff measure (57) is the natural tool to express "how close" two sets of points are. In order to make the results consistent, we further define a normalized error metric as

$$\varepsilon_{\mathcal{P}} = \frac{\mathcal{D}(\Lambda\{\mathcal{P}\}, \Lambda\{\mathcal{M}_1\})}{|\Lambda\{\mathcal{M}_1\}|} \quad (60)$$

where $|\Lambda\{\mathcal{M}_1\}|$ denotes the maximum magnitude among all Hamiltonian eigenvalues. The maximum deviation reported in Table I for all cases is on the order of machine precision, as expected. Since a real-valued state–space realization was used for all cases, we have $\mathcal{M}_1 = \overline{\mathcal{M}}_1$ and $\widehat{\mathcal{M}}_1 = \widetilde{\mathcal{M}}_1$, as confirmed by the numerical results. The last column in Table I reports the same error metric (60) applied to the full Hamiltonian eigenvalue set recovered as the (complex) square root of the eigenvalues of the half-size passivity matrix $\mathbf{P}_+$. Also in this case, the deviation is close to machine precision.

B. Eigenvector Characterization

In this section, we provide a validation for the Hamiltonian eigenvector characterization presented in Section III-E. For the same test cases of Section IV-A, we perform the following steps.

Step 1) The set $\Omega = \{j\omega_i, i = 1, \dots, n_i\}$ of purely imaginary eigenvalues of the Hamiltonian matrix $\mathcal{M}_1$ is extracted from the full set $\Lambda\{\mathcal{M}_1\}$.

Step 2) The eigenvectors $\boldsymbol{x}_i$ of $\mathcal{M}_1$ corresponding to each eigenvalue $j\omega_i$ are also computed via a general-purpose full eigensolver [30].

Step 3) The reconstruction $\boldsymbol{x}_i^+$ of the Hamiltonian eigenvectors based on the half-size passivity test matrix $\mathbf{P}_+$ are computed via (55).

Step 4) All true and reconstructed eigenvectors are normalized to have a unit norm.

Step 5) For each pair of true and reconstructed eigenvectors $(\boldsymbol{x}_i, \boldsymbol{x}_i^+)$, a constant phase shift is applied $\boldsymbol{x}_i^+$ so that $\angle(\boldsymbol{x}_i^+)_k = \angle(\boldsymbol{x}_i)_k$, where k is the component with the maximum magnitude.

As a result of above process, we can directly compare each true eigenvector with its reconstruction using the following error metric:

$$\epsilon_{\boldsymbol{x}} = \max_i \left\| \boldsymbol{x}_i^+ - \boldsymbol{x}_i \right\|_2 \quad (61)$$

Case	$\epsilon_{\boldsymbol{x}}$	$\theta_{\boldsymbol{x}}$	T_{full}	T_{half}	Speedup
A	7.5×10^{-11}	6.1×10^{-13}	24.18	3.21	7.52
B	3.6×10^{-8}	1.9×10^{-12}	103.0	13.3	7.74
C	2.3×10^{-7}	2.6×10^{-12}	13.29	1.88	7.06

where the standard energy norm is used, in addition to the standard residual vector norm

$$\theta_{\boldsymbol{x}} = \max_i \left\| \mathcal{M}_1 \boldsymbol{x}_i^+ - j\omega_i \boldsymbol{x}_i^+ \right\|_2 \qquad (62)$$

computed using the half-size eigenvector reconstructions. The results, reported in Table II, show a close to machine precision accuracy for the residual norm $\theta_{\boldsymbol{x}}$, whereas a slight precision loss is can be noted on $\epsilon_{\boldsymbol{x}}$. This can be explained by noting that, for cases B and C, some of the imaginary eigenvalues happen to be clustered with other Hamiltonian eigenvalues, thus leading to increased sensitivity [35], [36].

Table II also reports the CPU time (using a notebook with 2.0-GHz clock and 1-GB RAM) needed for the computation of eigenvectors using full-size (T_{full}) and half-size (T_{half}) processes. The speedup factor achieved by the half-size process approaches the ideal factor 8. Only a marginal overhead, needed for the postprocessing steps described in (53)–(55), reduces this speedup by a small factor. It should be noted that this overhead is proportional to the number of imaginary Hamiltonian eigenvalues (see Table I) and vanishes when the model is passive.

V. CONCLUSIONS

This paper has provided a complete and self-consistent theoretical framework for the passivity characterization of real-symmetric rational macromodels. This characterization is obtained as a set of purely algebraic tests based on the extraction of few eigenvalues and associated eigenvectors of suitable "half-size" test matrices. The main results extend previous characterizations by highlighting proper connection to classical Hamiltonian matrix theory. Finally, a reliable reduced-complexity process for the identification of passivity violation subbands has been presented, which requires a fraction of the CPU time with respect to standard techniques.

APPENDIX

A. Standard Hamiltonian Matrices

We report a sketch of the proof for Theorems 1 and 2. The derivations provide a constructive way for the derivation of the Hamiltonian matrices corresponding to a general rational macromodel $\mathbf{H}(s)$ in hybrid (admittance and impedance) and scattering representation, respectively.

Proof: Theorem 1 (hybrid, admittance, and impedance representations). Let us assume that δ is an eigenvalue of $\boldsymbol{\Psi}(j\omega_0)$. By definition,

$$\left[\mathbf{C}(j\omega_0\mathbf{I} - \mathbf{A})^{-1}\mathbf{B} + \mathbf{B}^H(-j\omega_0\mathbf{I} - \mathbf{A}^H)^{-1}\mathbf{C}^H \right.$$
$$\left. + \mathbf{D} + \mathbf{D}^H \right] \boldsymbol{v} = 2\delta\boldsymbol{v} \quad (63)$$

where $\boldsymbol{v}$ is the associated right eigenvector. Defining

$$\boldsymbol{r} = (j\omega_0\mathbf{I} - \mathbf{A})^{-1}\mathbf{B}\boldsymbol{v} \qquad (64)$$
$$\boldsymbol{q} = (-j\omega_0\mathbf{I} - \mathbf{A}^H)^{-1}\mathbf{C}^H\boldsymbol{v} \qquad (65)$$

we can express $\boldsymbol{v}$ via (63) as

$$\boldsymbol{v} = (2\delta\mathbf{I} - \mathbf{D} - \mathbf{D}^H)^{-1}(\mathbf{C}\boldsymbol{r} + \mathbf{B}^H\boldsymbol{q}). \qquad (66)$$

Substitution into (64) and (65) leads to

$$\mathcal{N}_\delta \begin{bmatrix} \boldsymbol{r} \\ \boldsymbol{q} \end{bmatrix} = j\omega_0 \begin{bmatrix} \boldsymbol{r} \\ \boldsymbol{q} \end{bmatrix} \qquad (67)$$

where $\mathcal{N}_\delta$ is defined as in (12), proving that $j\omega_0$ is an imaginary eigenvalue of the Hamiltonian matrix $\mathcal{N}_\delta$ and $[\boldsymbol{r}; \boldsymbol{q}]$ is the associated eigenvector. The converse is proved by repeating the same derivations in reverse order. ∎

Proof: Theorem 2 (scattering representations). Let us assume that γ is a singular value of $\mathbf{H}(j\omega_0)$. By definition,

$$\left[\mathbf{D} + \mathbf{C}(j\omega_0\mathbf{I} - \mathbf{A})^{-1}\mathbf{B} \right] \boldsymbol{u} = \gamma\boldsymbol{v} \qquad (68)$$
$$\left[\mathbf{D}^H + \mathbf{B}^H(-j\omega_0\mathbf{I} - \mathbf{A}^H)^{-1}\mathbf{C}^H \right] \boldsymbol{v} = \gamma\boldsymbol{u} \qquad (69)$$

where $\boldsymbol{u}$ and $\boldsymbol{v}$ are the left and right singular vectors, respectively. Defining

$$\boldsymbol{r} = (j\omega_0\mathbf{I} - \mathbf{A})^{-1}\mathbf{B}\boldsymbol{u} \qquad (70)$$
$$\boldsymbol{q} = (-j\omega_0\mathbf{I} - \mathbf{A}^H)^{-1}\mathbf{C}^H\boldsymbol{v} \qquad (71)$$

we can express the left and right singular vectors via (68) and (69) as

$$\begin{bmatrix} \boldsymbol{u} \\ \boldsymbol{v} \end{bmatrix} = \begin{bmatrix} -\mathbf{D} & \gamma\mathbf{I} \\ \gamma\mathbf{I} & -\mathbf{D}^H \end{bmatrix}^{-1} \begin{bmatrix} \mathbf{C}\boldsymbol{r} \\ \mathbf{B}^H\boldsymbol{q} \end{bmatrix}. \qquad (72)$$

Substitution into (70) and (71) leads to

$$\mathcal{M}_\gamma \begin{bmatrix} \boldsymbol{r} \\ \boldsymbol{q} \end{bmatrix} = j\omega_0 \begin{bmatrix} \boldsymbol{r} \\ \boldsymbol{q} \end{bmatrix} \qquad (73)$$

where $\mathcal{M}_\gamma$ is defined as in (13), proving that $j\omega_0$ is an imaginary eigenvalue of the Hamiltonian matrix $\mathcal{M}_\gamma$ and $[\boldsymbol{r}; \boldsymbol{q}]$ is the associated eigenvector. The converse is proven by repeating the same derivations in reverse order. ∎

B. Proof of Theorems 4 and 5

The constructive proofs below provide a derivation of the passivity matrices $\widehat{\mathcal{N}}_\delta$ and $\widehat{\mathcal{M}}_\gamma$ of (29) and (32), corresponding to a real-symmetric rational macromodel $\mathbf{H}(s)$ in admittance,

impedance and scattering representation, respectively. The proof for the other cases in the theorems are omitted.

Proof: Theorem 4 (admittance and impedance representations). Let us assume that δ is an eigenvalue of $\widehat{\Psi}(j\omega_0)$ in (23). By definition,

$$\left[\mathbf{C}(j\omega_0\mathbf{I} - \mathbf{A})^{-1}\mathbf{B} + \mathbf{C}(-j\omega_0\mathbf{I} - \mathbf{A})^{-1}\mathbf{B} + 2\mathbf{D}\right]\mathbf{v} = 2\delta\mathbf{v} \tag{74}$$

where $\mathbf{v}$ is the associated right eigenvector. Defining

$$\widehat{\mathbf{r}} = (j\omega_0\mathbf{I} - \mathbf{A})^{-1}\mathbf{B}\mathbf{v} \tag{75}$$

$$\widehat{\mathbf{q}} = (-j\omega_0\mathbf{I} - \mathbf{A})^{-1}\mathbf{B}\mathbf{v} \tag{76}$$

we can express $\mathbf{v}$ via (74) as

$$\mathbf{v} = (2\delta\mathbf{I} - 2\mathbf{D})^{-1}\mathbf{C}(\widehat{\mathbf{r}} + \widehat{\mathbf{q}}). \tag{77}$$

Substitution into (75) and (76) leads to

$$\widehat{\mathcal{N}}_\delta \begin{bmatrix} \widehat{\mathbf{r}} \\ \widehat{\mathbf{q}} \end{bmatrix} = j\omega_0 \begin{bmatrix} \widehat{\mathbf{r}} \\ \widehat{\mathbf{q}} \end{bmatrix} \tag{78}$$

where $\widehat{\mathcal{N}}_\delta$ is defined as in (29), proving that $j\omega_0$ is an imaginary eigenvalue of the passivity matrix $\widehat{\mathcal{N}}_\delta$ and $[\widehat{\mathbf{r}}; \widehat{\mathbf{q}}]$ is the associated eigenvector. The converse is proved by repeating the same derivations in reverse order. ∎

Proof: Theorem 5 (scattering representations). Let us assume that γ is a singular value of $\mathbf{H}(j\omega_0)$. Using (20), we have by definition

$$\left[\mathbf{D} + \mathbf{C}(j\omega_0\mathbf{I} - \mathbf{A})^{-1}\mathbf{B}\right]\mathbf{u} = \gamma\mathbf{v} \tag{79}$$

$$\left[\mathbf{D} + \mathbf{C}(-j\omega_0\mathbf{I} - \mathbf{A})^{-1}\mathbf{B}\right]\mathbf{v} = \gamma\mathbf{u} \tag{80}$$

where $\mathbf{u}$ and $\mathbf{v}$ are the left and right singular vectors, respectively. Defining

$$\widehat{\mathbf{r}} = (j\omega_0\mathbf{I} - \mathbf{A})^{-1}\mathbf{B}\mathbf{u} \tag{81}$$

$$\widehat{\mathbf{q}} = (-j\omega_0\mathbf{I} - \mathbf{A})^{-1}\mathbf{B}\mathbf{v} \tag{82}$$

we can express the left and right singular vectors via (79) and (80) as

$$\begin{bmatrix} \mathbf{u} \\ \mathbf{v} \end{bmatrix} = \begin{bmatrix} -\mathbf{D} & \gamma\mathbf{I} \\ \gamma\mathbf{I} & -\mathbf{D} \end{bmatrix}^{-1} \begin{bmatrix} \mathbf{C}\widehat{\mathbf{r}} \\ \mathbf{C}\widehat{\mathbf{q}} \end{bmatrix}. \tag{83}$$

Substitution into (81) and (82) leads to

$$\widehat{\mathcal{M}}_\gamma \begin{bmatrix} \widehat{\mathbf{r}} \\ \widehat{\mathbf{q}} \end{bmatrix} = j\omega_0 \begin{bmatrix} \widehat{\mathbf{r}} \\ \widehat{\mathbf{q}} \end{bmatrix} \tag{84}$$

where $\widehat{\mathcal{M}}_\gamma$ is defined as in (32), proving that $j\omega_0$ is an imaginary eigenvalue of the passivity matrix $\widehat{\mathcal{M}}_\gamma$, and $[\widehat{\mathbf{r}}; \widehat{\mathbf{q}}]$ is the associated eigenvector. The converse is proven by repeating the same derivations in reverse order. ∎

REFERENCES

[1] M. Celik, L. Pileggi, and A. Obadasioglu, *IC Interconnect Analysis*. Norwell, MA: Kluwer, 2002.

[2] M. Nakhla and R. Achar, "Simulation of high-speed interconnects," *Proc. IEEE*, vol. 89, no. 5, pp. 693–728, May 2001.

[3] B. Gustavsen and A. Semlyen, "Rational approximation of frequency responses by vector fitting," *IEEE Trans. Power Del.*, vol. 14, no. 3, pp. 1052–1061, Jul. 1999.

[4] B. Gustavsen, "Computer code for rational approximation of frequency dependent admittance matrices," *IEEE Trans. Power Del.*, vol. 17, no. 4, pp. 1093–1098, Oct. 2002.

[5] B. Gustavsen and A. Semlyen, "A robust approach for system identification in the frequency domain," *IEEE Trans. Power Del.*, vol. 19, no. 3, pp. 1167–1173, Jul. 2004.

[6] D. Deschrijver and T. Dhaene, "Rational modeling of spectral data using orthonormal vector fitting," in *Proc. 9th IEEE Signal Propag. Interconnects Workshop*, Garmisch-Partenkirchen, Germany, May 10–13, 2005, pp. 111–114.

[7] D. Deschrijver, B. Haegeman, and T. Dhaene, "Orthonormal vector fitting: A robust macromodeling tool for rational approximation of frequency domain responses," *IEEE Trans. Adv. Packag.*, vol. 30, no. 2, pp. 216–225, May 2007.

[8] S. Grivet-Talocia and M. Bandinu, "Improving the convergence of vector fitting in presence of noise," *IEEE Trans. Electromagn. Compat.*, vol. 48, no. 1, pp. 104–120, Feb. 2006.

[9] IdEM. ver. 2.4, Politech. Torino, Turin, Italy, 2006. [Online]. Available: www.emc.polito.it

[10] S. Grivet-Talocia, "On driving non-passive macromodels to instability," *Int. J. Circuit Theory Appl.*, vol. 37, pp. 863–886, 2009.

[11] T. Kailath, *Linear systems*. Englewood Cliffs, NJ: Prentice-Hall, 1980.

[12] M. R. Wohlers, *Lumped and Distributed Passive Networks*. New York: Academic, 1969.

[13] S. Boyd, L. El Ghaoui, E. Feron, and V. Balakrishnan, *Linear Matrix Inequalities in System and Control Theory*, ser. Studies in Appl. Math. Philadelphia, PA: SIAM, 1994.

[14] P. Triverio, S. Grivet-Talocia, M. S. Nakhla, F. Canavero, and R. Achar, "Stability, causality, and passivity in electrical interconnect models," *IEEE Trans. Adv. Packag.*, vol. 30, no. 4, pp. 795–808, Nov. 2007.

[15] S. Grivet-Talocia and A. Ubolli, "On the generation of large passive macromodels for complex interconnect structures," *IEEE Trans. Adv. Packag.*, vol. 29, no. 1, pp. 39–54, Feb. 2006.

[16] D. Saraswat, R. Achar, and M. Nakhla, "Global passivity enforcement algorithm for macromodels of interconnect subnetworks characterized by tabulated data," *IEEE Trans. Very Large Scale Integr. (VLSI) Syst.*, vol. 13, no. 7, pp. 819–832, Jul. 2005.

[17] C. P. Coelho, J. Phillips, and L. M. Silveira, "A convex programming approach for generating guaranteed passive approximations to tabulated frequency-data," *IEEE Trans. Comput.-Aided Design Integr. Circuits Syst.*, vol. 23, no. 2, pp. 293–301, Feb. 2004.

[18] H. Chen and J. Fang, "Enforcing bounded realness of S parameter through trace parameterization," in *12th IEEE Elect. Perform. Electron. Packag. Topical Meeting*, Princeton, NJ, Oct. 27–29, 2003, pp. 291–294.

[19] B. Dumitrescu, "Parameterization of positive-real transfer functions with fixed poles," *IEEE Trans. Circuits Syst. I, Fundam. Theory Appl.*, vol. 49, no. 4, pp. 523–526, Apr. 2002.

[20] B. Gustavsen and A. Semlyen, "Enforcing passivity for admittance matrices approximated by rational functions," *IEEE Trans. Power Syst.*, vol. 16, no. 1, pp. 97–104, Feb. 2001.

[21] B. Gustavsen, "Computer code for passivity enforcement of rational macromodels by residue perturbation," *IEEE Trans. Adv. Packag.*, vol. 30, no. 2, pp. 209–215, May 2007.

[22] B. Gustavsen, "Fast passivity enforcement of rational macromodels by perturbation of residue matrix eigenvalues," in *11th IEEE Signal Propag. Interconnects Workshop*, Ruta di Camogli, Genova, Italy, May 13–16, 2007, pp. 71–74.

[23] D. Saraswat, R. Achar, and M. Nakhla, "A fast algorithm and practical considerations for passive macromodeling of measured/simulated data," *IEEE Trans. Compon., Packag., Manuf. Technol.*, vol. 27, no. 1, pp. 57–70, Feb. 2004.

[24] S. Grivet-Talocia, "Passivity enforcement via perturbation of Hamiltonian matrices," *IEEE Trans. Circuits Syst. I, Reg. Papers*, vol. 51, no. 9, pp. 1755–1769, Sep. 2004.

[25] S. Grivet-Talocia, "An adaptive sampling technique for passivity characterization and enforcement of large interconnect macromodels," *IEEE Trans. Adv. Packag.*, vol. 30, no. 2, pp. 226–237, May 2007.

[26] A. Lamecki and M. Mrozowski, "Equivalent SPICE circuits with guaranteed passivity from nonpassive models," *IEEE Trans. Microw. Theory Tech.*, vol. 55, no. 3, pp. 526–532, Mar. 2007.

[27] S. Grivet-Talocia and A. Ubolli, "Passivity enforcement with relative error control," *IEEE Microw. Theory Tech.*, vol. 55, no. 11, pp. 2374–2383, Nov. 2007.

[28] S. Boyd, V. Balakrishnan, and P. Kabamba, "A bisection method for computing the H_∞ norm of a transfer matrix and related problems," *Math. Contr. Signals Syst.*, vol. 2, no. 3, pp. 207–219, Sep. 1989.

[29] G. H. Golub and C. F. van Loan, *Matrix Computations*, 3rd ed. Baltimore, MD: The Johns Hopkins Univ. Press, 1996.

[30] *"Matlab R2007b User's Guide"* The MathWorks, Natick, MA, 2007. [Online]. Available: www.mathworks.com

[31] F. Tisseur, "A chart of backward errors for singly and doubly structured eigenvalue problems," *SIAM J. Matrix Anal. Appl.*, vol. 24, no. 3, pp. 877–897, 2003.

[32] A. Semlyen and B. Gustavsen, "A half-size singularity test matrix for fast and realiable passivity assessment of rational models," *IEEE Trans. Power Del.*, vol. 24, no. 1, pp. 345–351, Jan. 2009.

[33] B. Gustavsen and A. Semlyen, "Fast passivity assessment for S-parameter rational models via a half-size test matrix," *IEEE Trans. Microw. Theory Tech.*, vol. 56, no. 12, pp. 2701–2708, Dec. 2008.

[34] M. Barnsley, *Fractals Everywhere*. New York: Academic, 1988.

[35] *Templates for the Solution of Algebraic Eigenvalue Problems: A Practical Guide*, Z. Bai, J. Demmel, J. Dongarra, A. Ruhe, and H. van der Vorst, Eds. Philadelphia, PA: SIAM, 2000.

[36] J. H. Wilkinson, *The Algebraic Eigenvalue Problem*. London, U.K.: Oxford Univ. Press, 1965.

Stefano Grivet-Talocia (M'98–SM'07) received the Laurea and Ph.D. degrees in electronic engineering from the Politecnico di Torino, Turin, Italy.

From 1994 to 1996, he was with the National Aeronautics and Space Administration (NASA)/Goddard Space Flight Center, Greenbelt, MD. He is currently an Associate Professor of circuit theory with Politecnico di Torino. His research interests are passive macromodeling of lumped and distributed interconnect structures, modeling and simulation of fields, circuits, and their interaction, wavelets, time-frequency transforms, and their applications. He has authored over 100 journal and conference papers.

Dr. Grivet-Talocia was an associate editor for the IEEE TRANSACTIONS ON ELECTROMAGNETIC COMPATIBILITY (1999–2001). He was a corecipient of the 2007 Best Paper Award of the IEEE TRANSACTIONS ON ADVANCED PACKAGING. He was also the recipient of the IBM Shared University Research (SUR) Award (2007, 2008 and 2009).